Journal of Solid Mechanics Vol. 12, No. 2 (2020) pp. 278-296
DOI: 10.22034/jsm.2019.582000.1381

Fundamental Solution and Study of Plane Waves in Bio-Thermoelastic Medium with DPL

R. Kumar [1,*], A.K. Vashishth [1], S. Ghangas [2]

[1]*Department of Mathematics, Kurukshetra University, Kurukshetra - 136119 Haryana, India*
[2]*Department of Mathematics, MDSD Girls College, Ambala City – 134002 Haryana, India*

Received 4 February 2020; accepted 26 March 2020

ABSTRACT

The fundamental solution of the system of differential equations in bio-thermoelasticity with dual phase lag (DPL) in case of steady oscillations in terms of elementary function is constructed and basic property is established. The tissue is considered as an isotropic medium and the propagation of plane harmonic waves is studied. The Christoffel equations are obtained and modified with the thermal as well as bio thermoelastic coupling parameters. These equations explain the existence and propagation of three waves in the medium. Two of the waves are attenuating longitudinal waves and one is non-attenuating transverse wave. The thermal property has no effect on the transverse wave. The velocities and attenuating factors of longitudinal waves are computed for a numerical bioheat transfer model with phase lag. The variation with frequency, thermal parameters, blood perfusion parameter and phase lag parameter are presented graphically. Also the reflection of plane wave from a stress free isothermal boundary of isotropic bio-thermoelastic half space in the context of DPL theory of thermoelasticity is studied. The amplitude ratios of various reflected waves are obtained and these amplitude ratios are further used to obtain the energy ratios of various reflected waves. These energy ratios are function of the angle of incidence and bio-thermoelastic properties of the medium. The expressions of energy ratios have been computed numerically for a particular model to show the effect of Poisson ratio, blood perfusion rate and phase lag parameters.

Keywords: Fundamental solution; Dual-phase-lag; Bio-thermoelasticity; Wave propagation; Energy ratios.

1 INTRODUCTION

THE construction of fundamental solution has great importance in many mathematical, physical and engineering problems. To investigate the boundary value problems in the theory of biothermomechanics, elasticity and

*Corresponding author.
E-mail address: rajneesh_kuk@rediffmail.com (R. Kumar).

thermoelasticity by potential method, it is necessary to construct a fundamental solution of the system of partial differential equations. Hetnarski [1-2] was the first to study the fundamental solution in the classical theory of coupled thermoelasticity. The fundamental solution in the theories of elastic mixtures and thermoelasticity was constructed by Svanadze [3]. Ciarletta et.al. [4] studied the fundamental solution in the theory of micropolar thermoelasticity for materials with voids. Svanadze [5-6] studied fundamental solutions of the equations of the theory of thermoelasticity with microtemperatures and double porosity. Scarpetta et al. [7] constructed fundamental solutions in the theory of thermoelasticity for solids with double porosity. Svanadze [8-9] constructed fundamental solutions in the theory of elasticity and thermoelasticity for solids with triple porosity respectively. Sharma et al. [10-11] investigated the plane wave and fundamental solution in electro-microstretch elastic and viscoelastic solids. Kumar and Kansal [15-16] investigated fundamental solution in the theories of thermo-microstretch elastic diffusive solid and micro-polar thermoelastic diffusion with void. Kumar et al. [12] examined fundamental solution in micropolar thermoelastic solid with void. Kumar and Kaur [17] studied plane wave and fundamental solution in heat conduction micro-polar fluid. Kumar et al. [14] presented plane wave fundamental solution in a modified couple stress generalized thermoelastic with mass diffusion. Kumar et al. [13] discussed some consideration for fundamental solution in micro-polar thermoelastic material with double porosity. Sharma [29] studied the propagation of thermoelastic wave in poroelastic medium and showed that three of the waves are attenuating longitudinal wave and one is non-attenuating transverse wave. Several authors have studied thermal-mechanical behaviors of soft tissues under thermal therapy. Xu and Lu [18] analyzed the non-Fourier thermo-mechanical behavior of skin tissue under surface heating boundary conditions. Shen et al. [19-20] developed a tissue damage model using Fourier bio-heat transfer equation. It shows that thermally induced mechanical deformation decreases the activation energy for protein denaturation, making soft tissue more easily to be damaged. Li et al. [21-22] developed a model to predict thermally induced mechanical deformation and thermal damage of soft tissue by combining the Fourier bio-heat transfer equation with the theory of linear thermo-elasticity. Panji et al. [31-32] investigated some problems on wave propagation in a homogeneous, isotropic elastic medium by boundary element method. Panji and Ansari [33] developed a direct half plane time boundary element method and applied to analyse the transient response of ground surface in the presence of arbitrarily shaped lined tunnels, embedded in a line elastic half space subjected to propagation/incident SH wave. Various authors (Sharma and Ansari [35]; Sharma [36]; Kumar and Gupta [37]; Saini [38]; Kumar et al. [39]) studied the reflection, refraction and transmission problems in different media and obtained amplitude ratios. Xu et al. [23] investigated the non-Fourier behavior of skin biothermomechanics. Li et al. [24] gave a new methodology for modeling of thermal-mechanical behaviors and associated damage of soft tissues during thermal ablation, where the modeling process combines non-Fourier bio-heat transfer, continuum mechanics, as well as non-rigid motion of dynamics to predict and analyze temperature distribution and thermal-induced mechanical deformations of soft tissues.

In this work, we constructed a fundamental solution of the bioheat transfer equation with thermo-elastic coupling and equations of motion. The fundamental solution is constructed for the case of steady oscillations. In second part of the paper, the plane wave propagation in bio-thermomechanical system with DPL model is discussed. Christoffel equations are obtained and modified with thermal as well as the thermoelastic coupling parameter. These equations explain the existence and propagation of three waves in the medium. It is found that there are two attenuating longitudinal waves and one non-attenuating transverse wave. The phase velocities and attenuation coefficients of two longitudinal waves are computed numerically and presented graphically for bio-thermomechanical model. The variation with the frequency, lagging time and thermal and blood perfusion parameters depicted graphically. Also the reflection of plane wave from a stress free isothermal boundary of isotropic bio-thermoelastic half space in the context of DPL theory of bio-thermoelasticity is studied. The amplitude ratios of various reflected waves are obtained and these amplitude ratios are further used to obtain the energy ratios of various reflected waves. The effect of bio-thermoelastic parameters on energy ratios is presented graphically.

2 BASIC EQUATIONS

Let $x=(x_1,x_2,x_3)$ be a point of the Euclidean three-dimensional space R^3 and t denotes the time variable, $t>0$. Bioheat transfer equation Pennes [25] considering coupled thermo-elastic effect can be described as:

$$\rho c\frac{\partial\hat{T}}{\partial t}+\beta T_0\frac{\partial e}{\partial t}=-\nabla.q+\omega_b\rho_b c_b(T_b-\hat{\theta})+q_m+q_{ext}, \tag{1}$$

$$e = \nabla.\hat{\mathbf{u}} \tag{2}$$

and $\hat{T} = \hat{\theta} - T_0$, $\hat{T}$ temperature increment, $\hat{\theta}$ tissue temperature, T_0 reference temperature, ρ is tissue density, ρ_b blood density, c tissue specific heat, c_b blood specific heat, ω_b blood perfusion rate, T_b the temperature of blood, T_0 the initial temperature, β the coefficient of thermal expansion, q_m the metabolic heat generation, q_{ext} the external heat source, $\hat{\mathbf{u}}$ the displacement vector, q heat flux vector and $\nabla = \left(\frac{\partial}{\partial x_1}, \frac{\partial}{\partial x_2}, \frac{\partial}{\partial x_3}\right)$. Single phase lag (SPL) constitutive relation is described by Cattaneo [26] and Vernotte [27] to incorporate lagging behavior in Fourier law as follows:

$$(1 + \tau_q \frac{\partial}{\partial t}) q = -k \frac{\partial \hat{T}}{\partial t}. \tag{3}$$

DPL constitutive relation is described by Tzou [28] and given as follows:

$$(1 + \tau_q \frac{\partial}{\partial t}) \nabla . q = -k\, (1 + \tau_T \frac{\partial}{\partial t}) \Delta \hat{T}. \tag{4}$$

where τ_q , τ_T are phase lag parameters and ∇ is Laplacian operator.

Using Eq. (4) in Eq. (1), we obtain the following bioheat transfer equation

$$k\, (1 + \tau_T \frac{\partial}{\partial t}) \Delta \hat{T} = \rho c (\frac{\partial \hat{T}}{\partial t} + \tau_q \frac{\partial^2 \hat{T}}{\partial t^2}) + \beta T_0 (\frac{\partial e}{\partial t} + \tau_q \frac{\partial^2 e}{\partial t^2}) - \omega_b \rho_b c_b (T_b - \hat{\theta}) + \tau_q \omega_b \rho_b c_b \frac{\partial \hat{T}}{\partial t} - (1 + \tau_q \frac{\partial}{\partial t})(q_m + q_{ext}). \tag{5}$$

Biologically, soft tissues are complex in terms of material compositions and structural formations. While soft tissue structure shows time-dependent, non-linear and anisotropic behaviors, in terms of small deformation caused by thermal load, soft tissues can be investigated by linear thermo-elastic models to a high precision.

We consider an isotropic and homogeneous bio-thermoelastic medium with the assumption $T_b = T_0$ and assume that the subscripts preceded by a comma denote partial differentiation with respect to the corresponding Cartesian coordinate, repeated indices are summed over the range (1,2,3) and the dot denotes differentiation w.r.t. time *t*.

From the constitutive elastic material law under thermal loads, the stress tensor σ_{lj} is related to the strain tensor and temperature and given as follows:

$$\sigma_{lj} = \mu(\hat{u}_{l,j} + \hat{u}_{j,l}) + \lambda \hat{u}_{k,k} \delta_{lj} - \beta \hat{T} \delta_{lj}, \tag{6}$$

where is the displacement components, and δ_{ij} is the Kronecker's symbol defined as:

$$\delta_{ij} = \begin{cases} 0, & \text{for} i \neq j \\ 1, & \text{for} i = j \end{cases}.$$

The governing equations of motion is

$$\sigma_{lj,j} = \rho(\ddot{\hat{u}}_l - \hat{F}_l^{(1)}), l = 1,2,3. \tag{7}$$

where $\hat{\mathbf{F}}^{(1)} = (\hat{F}_1, \hat{F}_2, \hat{F}_3) = (-\rho \hat{F}_1^{(1)}, -\rho \hat{F}_2^{(1)}, -\rho \hat{F}_3^{(1)})$.

The equations of motion expressed in terms of the displacement vector *u* and the temperature $\hat{T}$ is

$$(\lambda+\mu)\nabla\nabla\hat{u}+\mu\Delta\hat{u}-\beta\nabla\hat{T}-\rho\frac{\partial^2\hat{u}}{\partial t^2}=F^{(1)}. \tag{8}$$

Eq. (5) can be written as:

$$k\,\tau_{11}\Delta\hat{T}-(\rho c\tau_{12}-\omega_b c_b\rho_b\tau_{13})\hat{T}-\beta T_0\tau_{12}\nabla u=\hat{F}_4. \tag{9}$$

For steady oscillations $\hat{u}_l$, $\hat{T}$, $\hat{F}_j$ are postulated to have a harmonic time variation, that is,

$$(\hat{u}_l,\hat{T},\hat{F}_j)(x,t)=Re[(u_l,T_l,F_j)(x)e^{-i\omega t}] \qquad l=1,2,3,\ j=1,2,3,4 \tag{10}$$

Using Eq. (10) in Eqs. (8) and (9), we have

$$\begin{aligned}&(\mu\Delta+\rho\omega^2)u+(\lambda+\mu)\nabla div u-\beta\nabla T=F^{(1)},\\&[k\,\tau_{14}\Delta-(\rho c\tau_{15}-\omega_b c_b\rho_b\tau_{16})]T-\beta T_0\tau_{15}\nabla u=F_4.\end{aligned} \tag{11}$$

where ω is angular frequency, $\omega>0$; $\mathbf{F}^{(1)}=(F_1,F_2,F_3)$.

We introduce second order matrix differential operator with constant coefficients

$$A(D_{x,\omega})=(A_{ij}(D_x,\omega))_{4\times4}, \tag{12}$$

where,

$$\begin{aligned}&A_{ij}=(\mu\frac{\partial^2}{\partial x_i^2})+(\lambda+\mu)\frac{\partial^2}{\partial x_i x_j}+(\rho\omega^2)\delta_{ij},A_{i4}=-\beta\frac{\partial}{\partial x_i},A_{4j}=-\beta T_0\tau_{15}\\&A_{44}=k\,\tau_{14}\Delta-[\rho c\tau_{15}-\omega_b c_b\rho_b\tau_{16}],Dx=(\frac{\partial}{\partial x_1},\frac{\partial}{\partial x_2},\frac{\partial}{\partial x_3}),i,j=1,2,3.\end{aligned}$$

It can be easily seen that Eq. (11) can be rewritten in the following matrix form:

$$\mathrm{A(Dx,\omega)U(x)=F(x)}, \tag{13}$$

where $U=(u,T)$ and $F=(F_1,F_2,F_3,F_4)$ are four-component vector functions, $x\in R^3$.

3 FUNDAMENTAL SOLUTIONS

3.1 Fundamental solution of equations

Definition: The fundamental solution of Eq. (11), the fundamental matrix of operator $A(D_x,\omega)$ is the matrix $\Gamma(x,\omega)=(\Gamma_{ij}(x,\omega))_{4\times4}$, satisfying the following equation in the class of generalized functions

$$A(D_x,\omega)\Gamma(x,\omega)=\delta(x)J, \tag{14}$$

where $\delta(x)$ is the Dirac delta function and $J=(\delta_{ij})_{4\times4}$ is the unit matrix, $x\in R^3$.

Assume that $\mu k\,\tau_{14}\neq0$ and consider the following system of non homogeneous equations:

$$(\mu\Delta+\rho\omega^2)\mathrm{u}+(\lambda+\mu)\nabla\mathrm{div}\mathrm{u}-\beta \mathrm{T}_0\tau_{15}\nabla\mathrm{T}=\mathrm{F}^{(1)},$$
$$-\beta\nabla u+[k\,\tau_{14}\nabla-(\rho c\,\tau_{15}-\omega_b\,\rho_b c_b\,\tau_{16})]T=F_4. \tag{15}$$

As one may easily verify, the system (15) may be written in the following form

$$\mathrm{A}^{\mathrm{T}}(\mathrm{Dx},\omega)\mathrm{U}(\mathrm{x})=\mathrm{F}(\mathrm{x}), \tag{16}$$

where A^T is the transpose of matrix A, $F=(F_1,F_2,F_3,F_4)$ is a four-component vector function and $x\in R^3$.

Applying the operator div to the first equation of the system (15), we obtain the following system

$$(\mu_0\Delta+\rho\omega^2)\mathrm{div}\mathbf{u}-\beta \mathrm{T}_0\tau_{15}\Delta\mathrm{T}=\mathrm{div}\mathbf{F}^{(1)}, \tag{17}$$
$$-\beta\nabla u+[k\,\tau_{14}\Delta-(\rho c\,\tau_{15}-\omega_b\,\rho_b c_b\,\tau_{16})]T=F_4.$$

where $\mu_0=\lambda+2\mu$.

The system of Eq. (17), can be written as:

$$B(\Delta,\omega)V x)=\phi(x), \tag{18}$$

where, $\phi=(\phi_1,\phi_2)=(divF,F_4)$ are two-component vector function.

$$B(\Delta,\omega)=(B_{ij}(\Delta,\omega))_{2\times 2},\,B_{11}(\Delta,\omega)=\mu_0\Delta+\rho\omega^2,$$
$$B_{12}=-\beta T_0\tau_{15}\Delta,\,B_{21}=-\beta,B_{22}=k\,\tau_{14}\Delta-(\rho c\,\tau_{15}-\omega_b\,\rho_b c_b\,\tau_{16}).$$

We introduce the notation

$$\Lambda_1(\Delta,\omega)=\frac{1}{\mu k\,\tau_{14}}detB(\Delta,\omega). \tag{19}$$

It is easily seen that $\Lambda_1(-\xi,\omega)=0$ is a second degree algebraic equation and there exits two roots λ_1^2, λ_2^2 w.r.t. ξ. Then we have

$$\Lambda_1(\Delta,\omega)=\prod_{j=1}^{2}(\Delta+\lambda_j^2). \tag{20}$$

Eq. (19) imply

$$\Lambda_1(\Delta,\omega)V=\Phi, \tag{21}$$

where,

$$\Phi=(\Phi_1,\Phi_2),\,\Phi_j=\frac{1}{\mu_0 k\,\tau^{14}}\sum_{l=1}^{2}B_{lj}^{*}\Phi_l,\,l=1,2. \tag{22}$$

and B_{lj}^{*} is the co-factor of the element B_{lj} of the matrix B.

Now applying the operator $\Lambda_1(\Delta,\omega)$ to the first equation of the system (15) and taking into account Eq. (21), we obtain

$$\Lambda_2(\Delta,\omega)u = F, \tag{23}$$

where $\Lambda_2(\Delta,\omega) = \Lambda_1(\Delta,\omega)(\Delta + \frac{\rho\omega^2}{\mu}) = \Lambda_1(\Delta,\omega)(\Delta + \lambda_3^2)$, and

$$F = \frac{1}{\mu}[\Lambda_1(\Delta,\omega)F - (\lambda+\mu)\nabla\Phi_1 + \beta T_0\tau_{15}\nabla\Phi_2]. \tag{24}$$

On the basis of equation (21) and (23), we get

$$\Lambda(\Delta,\omega)U(x) = \tilde{\Phi}(x) \tag{25}$$

where $\tilde{\Phi} = (F,\Phi_2)$ is a four-component vector function and

$$\Lambda(\Delta,\omega) = (\Lambda_{ij}(\Delta,\omega))_{4\times4},$$
$$\Lambda_{11} = \Lambda_{22} = \Lambda_2, \Lambda_{33} = \Lambda_2, \Lambda_{44} = \lambda_1$$
$$\Lambda_{ij} = 0,\ for\ \ i \neq j \text{ and } i,j = 1,2,3,4$$

We introduce the notations

$$n_{l1}(\Delta,\omega) = \frac{-(\lambda+\mu)}{\mu_0 k\,\tau_{14}}B_{l1}^* + \frac{\beta T_0\tau_{15}}{\mu_0 k\,\tau_{14}}B_{l2}^*, n_{lm}(\Delta,\omega) = \frac{1}{\mu_0 k\,\tau_{14}}B_{lm}^*(\Delta,\omega). \tag{26}$$

In view of Eqs. (26), from Eqs. (22) and (24), we have

$$\begin{aligned} F &= \frac{1}{\mu}\Lambda_1(\Delta,\omega)F + \sum_{l=1}^{2} n_{l1}(\Delta,\omega)\nabla\Phi_l = [\frac{1}{\mu}\Lambda_1(\Delta,\omega)I + n_{11}(\Delta,\omega)\nabla div\,]F + n_{21}(\Delta,\omega)\nabla F_4 \\ \Phi_2 &= n_{l2}(\Delta,\omega)divF + n_{22}(\Delta,\omega)F_4 \end{aligned} \tag{27}$$

where $\mathbf{I} = (\delta_{ij})_{3\times3}$ is the unit matrix. Thus, from Eqs. (27) we have

$$\tilde{\Phi}(x) = L^T(D_x,\omega)F(x), \tag{28}$$

where

$$L(D_x,\omega) = (L_{ij}(D_x,\omega))_{4\times4},$$
$$L_{lj} = \frac{1}{\mu}\Lambda_1(\Delta,\omega)\delta_{ij} + n_{11}(\Delta,\omega)\frac{\partial^2}{\partial x_l \partial x_j}, {}_{j4} = \eta_{12}\frac{\partial}{\partial x_j}, L_{4j} = \eta_{21}\frac{\partial}{\partial x_j}, L_{44} = \eta_{22}. \tag{29}$$

By virtue of Eqs. (18) and (28) from (25), it follows that $\Lambda U = L^T A^T U$. It is obvious that $L^T A^T = \Lambda$ and, hence,

$$A(D_x,\omega)L(D_x,\omega) = \Lambda(\Delta,\omega). \tag{30}$$

We assume that , where $l,j = 1,2,3$ and $l \neq j$. Let

$$Y(x,\omega)=(Y_{ij}(x,\omega))_{4\times 4},$$
$$Y_{11}(x,\omega)=Y_{22}(x,\omega)=Y_{33}(x,\omega)=\sum_{j=1}^{3}\eta_{2j}\gamma^{(j)}(x,\omega) \tag{31}$$
$$Y_{44}(x,\omega)=\sum_{j=1}^{3}\eta_{1j}\gamma^{(j)}(x,\omega), Y_{ij}(x,\omega)=0, \text{for}, i\neq j, i,j=1,2,3,4.$$

where

$$\gamma^{(j)}(x,\omega)=-\frac{e^{i\lambda_j|x|}}{4\pi|x|}, \tag{32}$$

Is the fundamental solution of the Helmholtz's equation, i.e. $(\Delta+\lambda_j^2)\gamma^{(j)}(x,\omega)=\delta(x)$ and

$$\eta_{11}=(\lambda_2^2-\lambda_1^2)^{-1}, \eta_{12}=(\lambda_1^2-\lambda_2^2)^{-1}, \tag{33}$$

$$\eta_{21}=(\lambda_2^2-\lambda_1^2)^{-1}(\lambda_3^2-\lambda_1^2)^{-1}, \eta_{22}=(\lambda_1^2-\lambda_2^2)^{-1}(\lambda_3^2-\lambda_2^2)^{-1}, \eta_{23}=(\lambda_1^2-\lambda_3^2)^{-1}(\lambda_2^2-\lambda_3^2)^{-1}, \tag{34}$$

Lemma: The matrix $Y(x,\omega)$ is the fundamental solution of the operator $\Lambda(\Delta,\omega)$, that is,

$$\Lambda(\Delta,\omega)Y(x,\omega)=\delta(x)J, \tag{35}$$

Proof: It is suffices to show that Y_{11} and Y_{44} are the fundamental solutions of operators $\Lambda_2(\Delta)$ and $\Lambda_1(\Delta)$, respectively, i.e.

$$\begin{aligned}\Lambda_2(\Delta,\omega)Y_{11}(x,\omega)=\delta(x)\\ \Lambda_1(\Delta,\omega)Y_{44}(x,\omega)=\delta(x)\end{aligned} \tag{36}$$

Taking into account the equalities

$$\sum_{j=1}^{2}\eta_{1j}=\eta_{11}+\eta_{12}=0, \text{and } \eta_{12}(\lambda_1^2-\lambda_2^2)=1$$
$$(\Delta+\lambda_l^2)\gamma^{(j)}(x,\omega)=\delta(x)+(\lambda_l^2-\lambda_j^2)\gamma^{(j)}(x,\omega),$$

We have

$$\begin{aligned}\Lambda_1(\Delta,\omega)Y_{44}(x,\omega) &=\prod_{j=1}^{2}(\Delta+\lambda_j^2)\sum_{j=1}^{2}\eta_{ij}\gamma^{j}(x,\omega)\\ &=(\Delta+\lambda_1^2)(\Delta+\lambda_2^2)[\eta_{11}\gamma^{1}(x,\omega)+\eta_{12}\gamma^{2}(x,\omega)]\\ &=(\Delta+\lambda_2^2)\sum_{j=1}^{2}\eta_{1j}[\delta(x)+(\lambda_1^2-\lambda_j^2)\gamma^{(j)}(x,\omega)]\\ &=(\Delta+\lambda_2^2)\sum_{j=1}^{2}\eta_{1j}\gamma^{j}(x,\omega)]=\delta(x).\end{aligned} \tag{37}$$

Similarly,

$$\Lambda_2(\Delta,\omega)Y_{44}(x,\omega)=\delta(x). \tag{38}$$

We introduce the matrix

$$\Gamma(x,\omega)=L(D_x,\omega)Y(x,\omega). \tag{39}$$

Using Eq. (30) and (34) from (35), we get

$$A(D_x,\omega)\Gamma(x,\omega)=A(D_x,\omega)L(D_x,\omega)Y(x,\omega)=\Lambda(\Delta,\omega)Y(x,\omega)=\delta(x)J. \tag{40}$$

Hence, $\Lambda(x,\omega)$ is the solution to Eq. (14).

Theorem: The matrix $\Gamma(x,\omega)$ defined by Eq. (39) is the fundamental solution of Eq. (11), where the matrices $L(D\ x,\omega)$ and $Y(x,\omega)$ are given by formulas (29) and (31), respectively.

Each element $\Gamma_{ij}(x,\omega)$ of the matrix $\Gamma(x,\omega)$ is represented in the following form:

$$\begin{aligned}\Gamma_{ij}(x,\omega) &= L_{ij}(D_x,\omega)Y_{11}(x,\omega),\\ \Gamma_{lm}(x,\omega) &= L_{lm}(D_x,\omega)Y_{44}(x,\omega),\\ l &= 1,2,3,4.\end{aligned} \tag{41}$$

3.2 Basic property of the matrix $\Gamma(x,\omega)$

Property: Each column of the matrix $\Gamma(x,\omega)$ is a solution of the homogeneous equation

$$A(D_x,\omega)\Gamma(x,\omega)=0$$

at every point $x\in R^3$ except the origin.

4 PLANE WAVE SOLUTION

We consider equation of motion and bioheat transfer equation in the absence of body force and heat source as:

$$\begin{aligned}&(\lambda+\mu)\hat{u}_{k,ik}+\mu\hat{u}_{i,kk}-\beta\hat{T}_{,i}-\rho\ddot{\hat{u}}_i=0,\\ &k(1+\tau_T\frac{\partial}{\partial t})\nabla^2\hat{T}-[\rho c(\frac{\partial}{\partial t}+\tau_q\frac{\partial^2}{\partial t^2})-\omega_b\rho_b c_b(1+\tau_q\frac{\partial}{\partial t})]\hat{T}-\beta T_0(\frac{\partial}{\partial t}+\tau_q\frac{\partial^2}{\partial t^2})\hat{u}_{j,j}=0.\end{aligned} \tag{42}$$

For harmonic solution of Eq. (42) for the propagation of plane waves, we assume

$$(\hat{u}_j,\hat{T}-T_0)=(U_j,\Gamma)\exp(i\omega(p_k x_k-t)), \tag{43}$$

where ω is angular frequency and (p_1,p_2,p_3) is slowness vector. In terms of the phase velocity *V*, slowness is written as $(p_1,p_2,p_3)=\frac{N}{V}$. The row matrix $N=(n_1,n_2,n_3)$ represents the direction of phase propagation. The vectors (U_1,U_2,U_3) defines the polarization for the motions of the solids particles. Substituting Eq. (43) in Eq. (42) yields

$$
\begin{aligned}
T &= T_0 + G n_k u_k , \\
G &= \frac{i\,\omega T_0 V\,\beta\tau}{k - \rho c \tau V^2}, \\
\tau &= \tau_0 + \frac{i}{\omega},
\end{aligned}
\tag{44}
$$

Relates the temperature (T) and particle displacement in the medium. The other subsystem is

$$AU = 0, \tag{45}$$

$$A = (\lambda + \mu - \beta g V^2) N^T N + (\mu - \rho V^2) I , \tag{46}$$

where I is the identity matrix of order three and N^T denotes the transpose of row matrix N. The later subsystem is resolved into the following eigen system

$$[aN^T N + b(I - N^T N)]U = 0, \tag{47}$$

where

$$a = (\lambda + 2\mu - \beta g V^2 - \rho V^2), \tag{48}$$

$$b = \mu - \rho V^2, \tag{49}$$

$$g = \frac{T_0 \beta\tau}{k\,\tau_{14} - \tau_{T2} V^2}. \tag{50}$$

The eigensystem (47) explains the propagation phenomenon in the medium and may be called the generalized Christoffel equations for thermoelastic wave propagation in the considered medium.

Non-trivial solution for Christoffel Eq. (47) is ensured by vanishing the determinant of the coefficient matrix $aN^T N + b(I - N^T N)$. For $b = 0$, we get a relation

$$V = \sqrt{\frac{\mu}{\rho}}, \tag{51}$$

with polarization U normal to propagation direction N. Hence this defines the phase velocity of a non-attenuating transverse wave in the medium. The other relation, $a = 0$, is solved into

$$(\lambda + 2\mu) - \beta g V^2 - \rho V^2 = 0. \tag{52}$$

For $k \neq \rho c \tau V^2$, the Eq. (52) is solved into a quadratic equation in V^2. This quadratic equation is written as:

$$C_0 V^4 + C_1 V^2 + C_2 = 0, \tag{53}$$

Two roots of quadratic Eq. (53) explain the existence and propagation of two longitudinal waves in thermoelastic solid. The relaxation time parameter τ is frequency dependent complex number. This implies that the roots of Eq. (53) are complex and hence the longitudinal waves in the medium are attenuating waves.

5 REFLECTION AT PLANE BOUNDARY

This study aims to analyse the propagation and attenuation of three reflected waves at the free plane surface of a bio-thermoelastic medium. The half space $x_3 \geq 0$ is considered as the bio-thermoelastic solid with depth increasing along the x_3-direction. The plane $x_3 = 0$ is the surface of the medium. The propagation and attenuation of waves are considered in a $x_1 - x_3$ plane. In this plane an incident wave travels towards the surface making an angle θ with the x_3 axis.

The components of displacement are given by

$$u_1 = \frac{\partial \phi}{\partial x_1} - \frac{\partial \psi}{\partial x_3}, \tag{54}$$

$$u_3 = \frac{\partial \phi}{\partial x_3} + \frac{\partial \psi}{\partial x_1}, \tag{55}$$

where ϕ and ψ satisfy the following wave equations

$$(\nabla^2 + \frac{\omega^2}{V_i^2})\phi_i = 0, i = 1,2. \tag{56}$$

$$\mu \nabla^2 \psi = \rho \frac{\partial^2 \psi}{\partial t^2}, \tag{57}$$

where $\phi = \phi_1 + \phi_2$ and V_i are velocities of two longitudinal wave obtained from the Eq. (53).

The potential functions can be written as:

$$(\phi, T) = \sum_1^2 (1, n_i)(B_i^0 e^{(A_i^0.r)} e^{i(P_i^0.r - \omega t)} + B_i^1 e^{(A_i^1.r)} e^{i(P_i^1.r - \omega t)}), \tag{58}$$

$$\psi = B_3^0 e^{(A_3^0.r)} e^{i(P_3^0.r - \omega t)} + B_3^1 e^{(A_3^1.r)} e^{i(P_3^1.r - \omega t)}, \tag{59}$$

where

$$n_i = \frac{-(\lambda + 2\mu)\omega^2 + \rho \omega^2 V_i^2}{\beta V_i^2}.$$

The coefficients B_i^0, $i = 1,2,3$ are the amplitudes of the incident *P*, *T* and SV wave respectively and the coefficients B_i^1, $i = 1,2,3$ are the amplitudes of the reflected *P*, *T* and SV wave respectively. The propagation vector P_i^0 and P_i^1 , and the attenuation vector A_i^0 and A_i^1 are given by

$$P_i^0 = k_R \hat{x}_1 - d_{iR} \hat{x}_3, P_i^1 = k_R \hat{x}_1 + d_{iR} \hat{x}_3, \tag{60}$$

$$A_i^0 = -k_I \hat{x}_1 + d_{iI} \hat{x}_3, A_i^1 = -k_I \hat{x}_1 - d_{iI} \hat{x}_3, \tag{61}$$

where

$$d_i = d_{iR} + id_{iI} = p.v.(\frac{\omega^2}{V_i^2} - k_R^2), i = 1,2,3. \tag{62}$$

$\hat{x}_1$ and $\hat{x}_3$ denotes the denote the unit vectors propagating in the x_1 and x_3 directions, respectively, and $k = k_R + ik_I$ is the complex wave number. The subscripts R and I denote the real and imaginary parts of the corresponding complex number, and p.v. stands for the principal value of the complex quantity derived from square root.

5.1 Boundary conditions

Three boundary conditions are required to be satisfied at the plane $x_3 = 0$.

$$\begin{aligned} &(i)\ \sigma_{33} = 0, \\ &(ii)\ \sigma_{31} = 0, \\ &(ii)\ T = 0. \end{aligned} \tag{63}$$

Making use of potentials given by Eqs. (58) and (59), we find that the boundary conditions are satisfied if and only if

$$k_R = \frac{\omega\sin(\theta)}{V} = \frac{\omega\sin(\theta_1)}{V_1} = \frac{\omega\sin(\theta_2)}{V_2} = \frac{\omega\sin(\theta_3)}{V_3}, \tag{64}$$

where V=V_1 ; for incident *P*-wave, V_2; for incident *T*-wave, V_3; for incident SV-wave.

Using the boundary conditions given by Eq. (63) and with the aid of Eqs. (6) and (47), we get a system of three non-homogeneous equations which can be written as:

$$\sum_{i=1}^{3} a_{ij} Z_j = Y_i, \tag{65}$$

where Z_j , $j = 1,2,3$ are the ratios of amplitudes of reflected *P*, reflected *T*, and reflected SV- waves to that of amplitude of incident wave.

$$\begin{aligned} &a_{1i} = (\lambda + 2\mu)d_i^2 + \lambda k^2, \text{ for } i=1,2, a_{13} = 2\mu k d_3, \\ &a_{2i} = 2kd_i, \text{ for } i=1,2, a_{23} = \left(k^2 - d_3^2\right), \\ &a_{3i} = 1, \text{ for } i=1,2, a_{33} = 0. \end{aligned}$$

The coefficients Y_i , $i = 1,2,3$ on the right side of the Eq. (64) are given by [labe l=()]

1. For incident *P*-wave $Y_1 = -a_{11}$, $Y_2 = a_{21}$, $Y_3 = -a_{31}$.
2. For incident *T*-wave $Y_1 = -a_{12}$, , $Y_3 = -a_{32}$.
3. For incident SV-wave $Y_1 = a_{13}$, $Y_2 = -a_{23}$, $Y_3 = a_{33}$.

5.2 Energy ratios

Distribution of incident energy among different reflected waves is considered across a surface element of unit area at the plane $x_3 = 0$. The scalar product of surface traction and particle velocity per unit area, denoted by P^*, represents the rate at which the energy is communicated per unit surface area per unit time. For a surface with normal along the x_3 direction, the average energy flux is represented through the components P_e^* given by

$$<P_e^*>= Re(\sigma_{31}^{(e)})Re(\dot{u}_1^e)+Re(\sigma_{33}^{(e)})Re(\dot{u}_3^{(e)}). \tag{66}$$

Following Achenbach [34] , for any two complex functions f and g, we have

$$(Re(f\,).Re(g)) = \frac{1}{2}Re(f\,.\bar{g}). \tag{67}$$

The energy ratios $E_i\ (i\ = 1,2,3)$, for the reflected P, T and SV waves, respectively, are defined as follows:

$$E_i\ = -\frac{(P_{ei}^*)}{P_{e0}^*}, (i\ = 1,2,3), \tag{68}$$

where

$$P_{e0}^* = \frac{1}{2}(\lambda+2\mu)Re((d_1^2+k^2)d_1\omega)\,|\,B_1^0\,|^2, \tag{69}$$

$$P_{e1}^* = -\frac{1}{2}(\lambda+2\mu)Re((d_1^2+k^2)d_1\omega)\,|\,B_1^1\,|^2, \tag{70}$$

$$P_{e2}^* = -\frac{1}{2}(\lambda+2\mu)Re((d_2^2+k^2)d_2\omega)\,|\,B_2^1\,|^2, \tag{71}$$

$$P_{e3}^* = -\frac{1}{2}\mu Re((k^2+d_3^2)d_3\omega)\,|\,B_3^1\,|^2\ . \tag{72}$$

The expression given by Eqs. (69)-(71) are calculated when P-wave is incident.

6 RESULTS AND DISCUSSION

Three waves are found in considered isotropic medium. Two of these are attenuating longitudinal waves and one non-attenuating transverse wave. For the complex velocity ($V\ = V_R\ + iV_I$), phase velocity and attenuation coefficient are defined as $V\ = \frac{V_R^2+V_I^2}{V_R^2}$ and $Q^{-1} = \frac{img(1/V^2)}{Re(1/V^2)}$ respectively.

The computation has been done using MATLAB (R2016a) software and results are presented graphically. Only the parameters whose values differs from reference value are indicated in figures. The selected referenced value for phase velocities and attenuation coefficients are given in the Table 1.

Table 1
Tissue parameters and constants

Parameters	Units	Values
Density ρ	$kg.m^{-3}$	1060
Specific heat c	$J.kg.^{-1}K.^{-1}$	4192
Thermal conductivity k	$W.m^{-1}.K^{-1}$	0.613
Thermal expansion coefficient α	$^{\circ}C^{-1}$	1×10^{-4}
Young's modulus E	Pa	0.1×10^{4}

Poisson's ratio ν		0.48
Blood perfusion rate ω_b	$Kg.m^{-3}s^{-1}$	0.5
Arterial temperature T_b	$^{\circ}C$	37
Blood specific heat c_b	$Jkg^{-1\circ}C^{-1}$	3600
Phase lag time τ_q ,	s	8,16

Fig. 1 shows the phase velocity and attenuation quality coefficient of PV_1 and PV_2 waves. From Fig. 1(a) it is clear that phase velocity has slight change as frequency (ω) increases but significant effect of ω_b has observed on phase velocity. As the value of ω_b increases phase velocity profile decreases. The phase velocity of () wave is much slower than the PV_1 wave as in Fig. 1(b). As frequency ω increases phase velocity () also increases and effect of blood perfusion parameter (ω_b) is observed. Fig. 1(c) shows the attenuation coefficient (AQ_1) decreases for and for $\omega > 0.5$ it increases. In Fig. 1(d) attenuation coefficient (AQ_2) is depicted. It is clear that it shows oscillating behavior for small value of frequency (ω), but for large value of frequency (ω) it shows constant behavior.

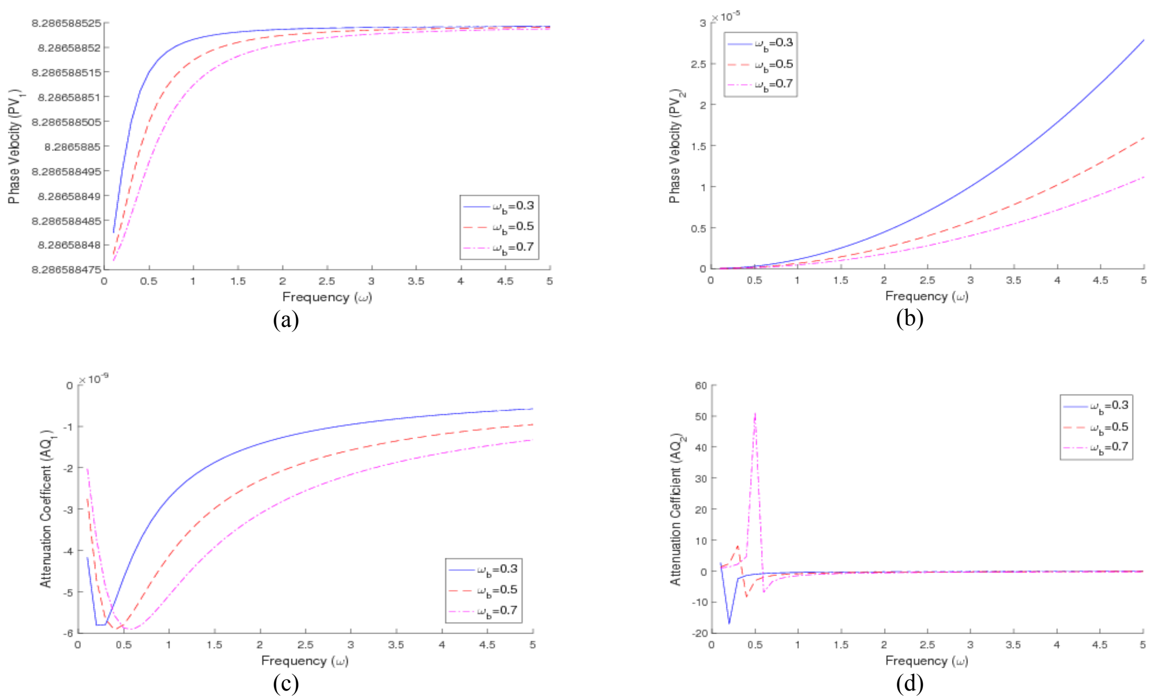

Fig.1
Effect of blood perfusion rate ω_b on phase velocities and attenuation coefficients.

Fig. 2 shows the variation in phase velocities (PV_1, PV_2) and attenuation coefficients (AQ_1, AQ_2) for different values of lagging times. From Fig. 2(a) and Fig. 2(b) it is clear that as the value of phase lag parameter τ_q increases phase velocity profile of PV_1 and PV_2 waves decreases. Fig. 2(c) shows that the profile of attenuation coefficient AQ_1 decreases as the lagging time (τ_q) increases. Fig. 2(d) shows that profile of attenuation coefficients AQ_2 remains stationary for $\geq \omega \leq 2$, for $2 < \omega < 4$ it shows oscillatory behavior and for $\omega > 4$ it again shows stationary behavior when $\tau_q < \tau_T$. When $\tau_q = \tau_T$ and $\tau_q > \tau_T$ the profile of attenuation coefficient AQ_2 is almost a straight line. Thus, we observed the significant effects of phase lag on phase velocities and attenuation coefficients of both the longitudinal waves.

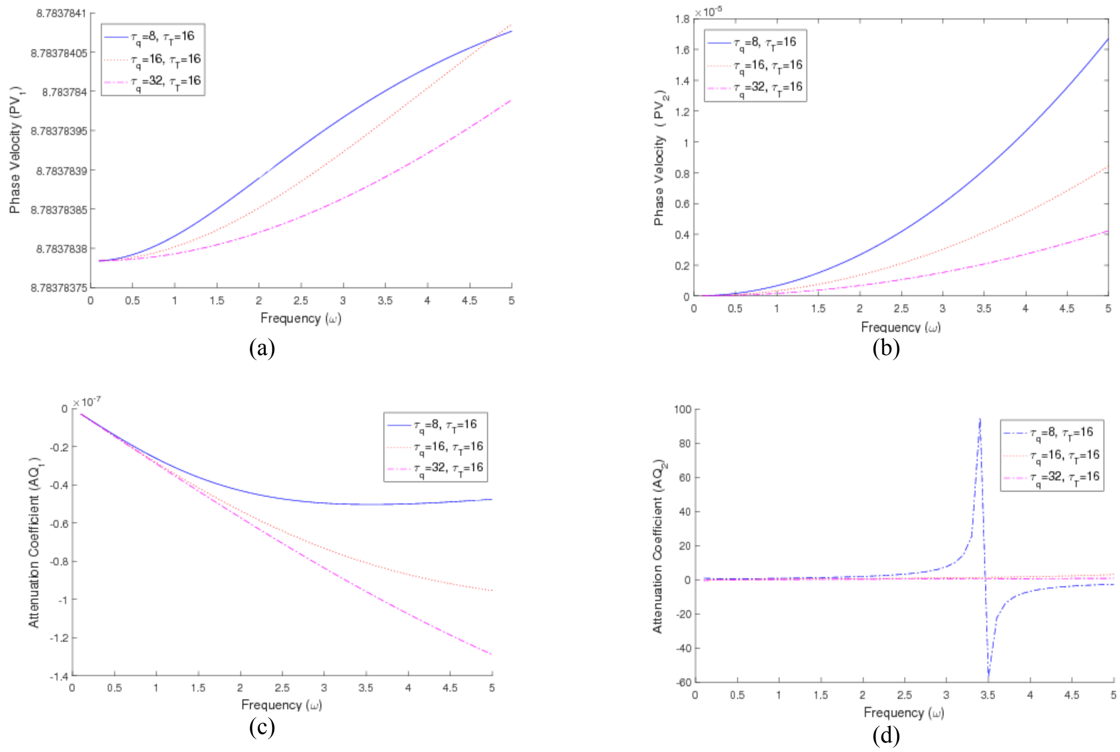

Fig.2
Variation in phase velocities and attenuation coefficients along frequency (ω) for different values of lagging time.

Fig. 3 shows the variation in phase velocities ($(PV_1), PV_2$) and attenuation coefficients (AQ_1, AQ_2) along Young's modulus for different value of Poisson's ratio (ν). From Fig. 3(a) it is clear that phase velocity (PV_1) increase monotonically as the value of Young's modulus increases and as the value of Poisson's ratio increases phase velocity increases. Phase velocity (PV_2) has oscillatory behavior as Young's modulus E increases as shown in Fig. 3(b). Fig. 3(c) shows that attenuation coefficient (AQ_1) decreases as the value of Young's modulus increases and attenuation coefficient is greater for smaller value of Poisson's ration (ν). Fig. 3(d) shows oscillatory behavior of attenuation coefficient (AQ_2). Thus, it is clear that phase velocities and attenuation coefficients are affected by Young's modulus and Poisson's ratio.

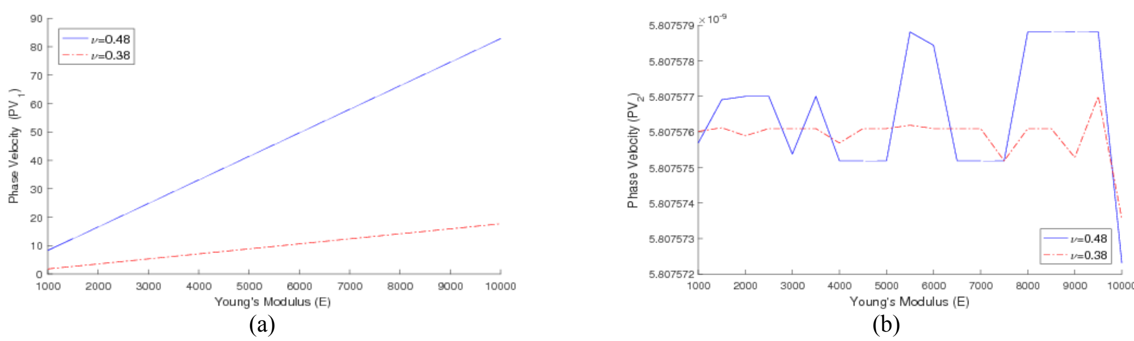

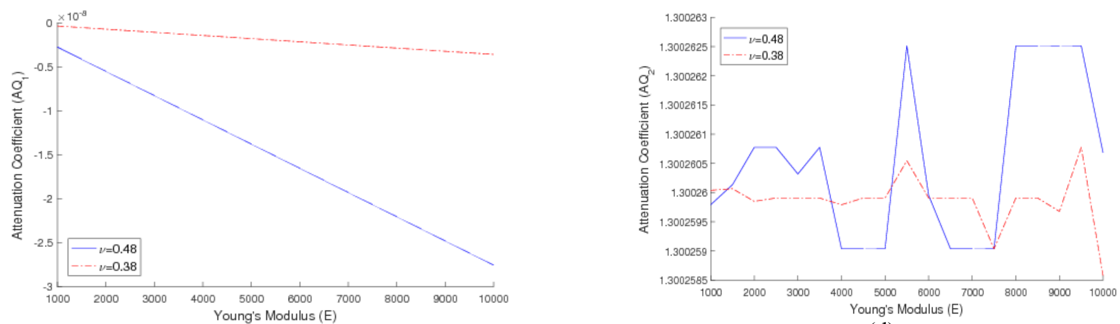

(c) (d)

Fig.3
Variation in phase velocities and attenuation coefficeints along Young’s modulus (E) for different values of Poission’s ratio (υ).

Fig. 4 shows the variation in energy ratio along the incident angle (θ) for different values of Poisson’s ratio (ν). The value of energy ratio E_1 increases as Poisson’s ratio ν increases. As Poisson’s ratio increases the value of E_1 gets closer to each other. Also for all angle of incidence the value of E_1 decreases. For initial angle of incidence value of E_2 are very close to each other and as the angle of incidence increases $\theta > 15$ it increases monotonically for all values of the Poisson’s ratio. The value of E_3 increases monotonically for all values of Poisson’s ratio with all angle of incidence. The value of E_2 and E_3 get decreased as Poisson’s ratio increases with all angle of incidence.

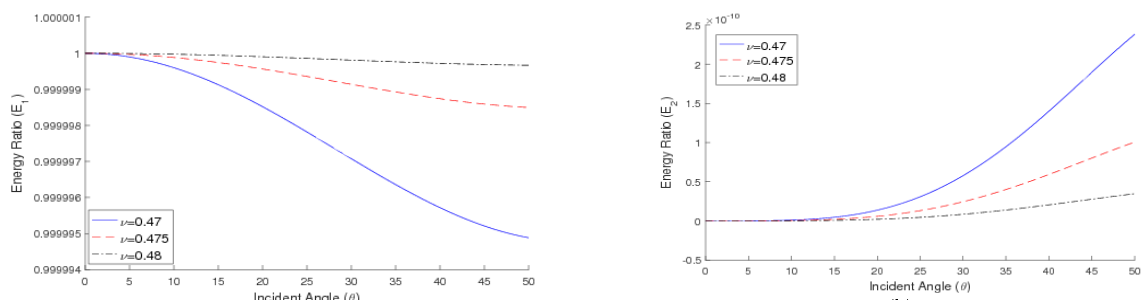

(a) (b)

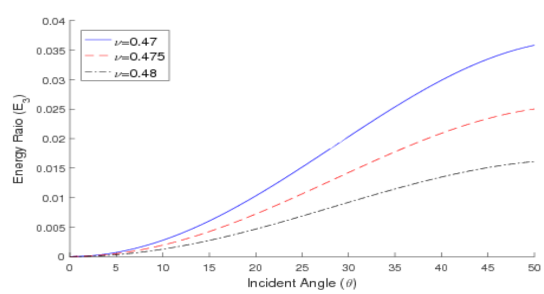

(c)

Fig.4
Variation in energy ratios (E_1, E_2, E_3) for different values of Poission’s ratio (ν).

It is noticed that from Fig. 5 and Fig. 6 that only energy ratio E_2 is affected by blood perfusion rate (ω_b) and phase lag parameters (τ_q, τ_T).

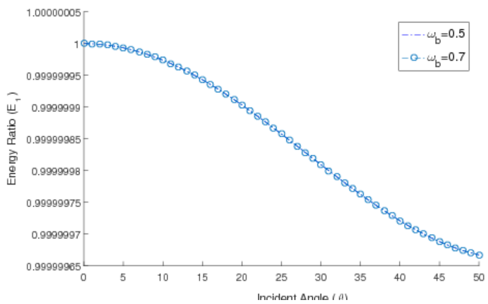

(a)

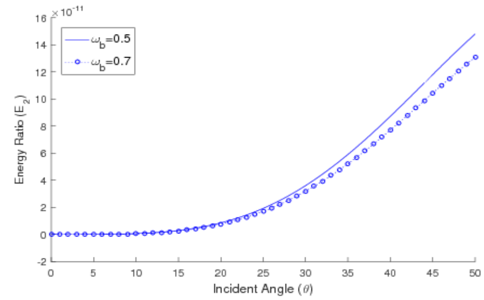

(b)

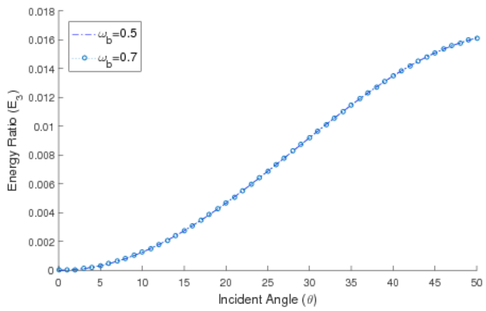

(c)

Fig.5
Variation in energy ratios (E_1, E_2, E_3) for different values of blood perfusion rate (ω_b).

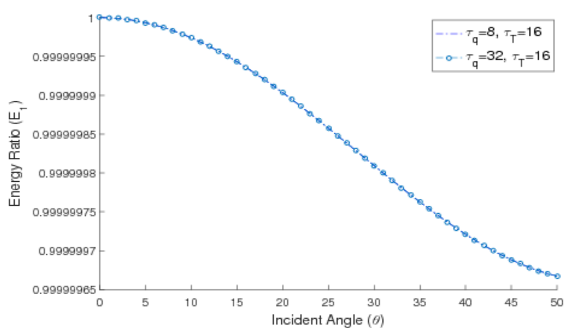

(a)

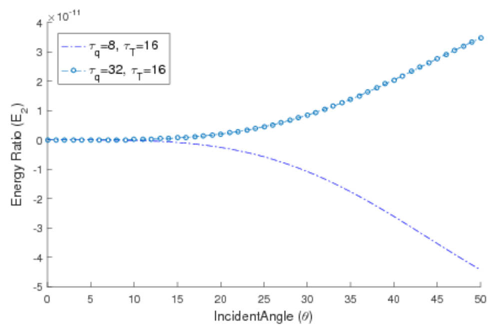

(b)

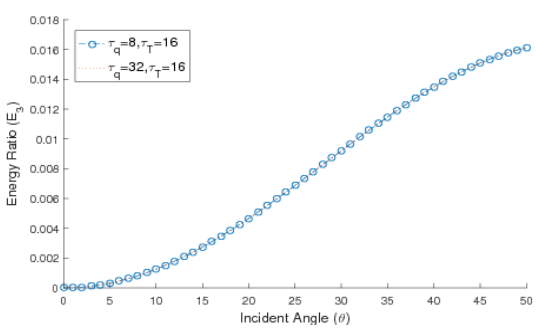

(c)

Fig.6
Variation in energy ratios (E_1, E_2, E_3) for different values of phase lag parameters τ_q and τ_T .

7 CONCLUSION

The fundamental solution of the system of equations in the theory of bio-thermo-elasticity in case of steady oscillations in terms of elementary function has been constructed. The fundamental solution $\Gamma(x,\omega)$ of the system (11) make it possible to investigate three dimensional boundary value problem of bio-thermomechanics by potential method Kapradze et al. [30]. This type of study is useful due to its application in biomedical and bioengineering. In later part of the paper study of waves in tissues is investigated which is a significant problem. The existence and propagation of three waves is found. From these waves we found that one is transverse wave and two are longitudinal waves. The effects of blood perfusion parameter, lagging time, frequency and Young's modulus is observed. In the last section of the paper a mathematical treatment has been presented to explore the angle of incidence on wave propagation in a two dimensional model of bio-thermoelasticity with DPL . The problem has been solved theoretically and explained through a specific model. Though the figures are self explanatory in depicting the different peculiarities which occur in the propagation of waves. Yet the following remark may be added:

It is concluded that the behavior and variation of E_1 and E_3 are opposite to each other for considered value of Poisson ratio and only energy ratio E_2 is effected by the blood perfusion rate and phase lag parameters. The problem assumes great significance when we consider the real behavior of material characteristic with appropriate geometry of the model. Thus, it is concluded that the problem discussed will provide useful information for experimental researchers working in the field of biomedical, geophysics and earth-quack engineering.

ACKNOWLEDGMENT

The third author is thankful to the Council of Scientific and Industrial Research (CSIR), India, for the financial support under the SRF (21/06/2015/(i)EU-V) scheme.

APPENDIX

$$\tau_{11} = (1+\tau_T \frac{\partial}{\partial t}),\ \tau_{12} = (\frac{\partial}{\partial t} + \tau_q \frac{\partial^2}{\partial t^2}),$$

$$\tau_{13} = (1+\tau_q \frac{\partial}{\partial t}),\ F = -\rho F^{(1)}$$

$$\hat{F}_4 = -\tau_{13}\hat{s},\ \hat{s} = q_m + q_{ext}$$

$$\tau_{14} = (1+\tau_T (-i\,\omega)),$$

$$\tau_{15} = ((-i\,\omega + \tau_q (-i\,\omega)^2)),$$

$$\tau_{16} = (1+\tau_q (-i\,\omega)),$$

$$C_0 = \rho\tau_{T2},$$

$$C_1 = -[(\lambda+2\mu)\tau_{T2} + T_0\beta^2\tau + \rho k\,\tau_{14}],$$

$$C_2 = (\lambda+2\mu)k\,\tau_{14},$$

$$\tau_{T2} = \rho c + \frac{\omega_b \rho_b c_b \tau}{i\,\omega}.$$

REFERENCES

[1] Hetnarski R.B., 1964, Solution of the coupled problem of thermoelasticity in form of a series of functions, *Archives of Mechanics* **16**: 23-31.

[2] Hetnarski R.B., 1964, The fundamental solution of the coupled thermoelasticity problems for small times, *Archives of Mechanics* **16**: 919-941.

[3] Svanadze M., 1996, The fundamental solution of the oscillation equations of the thermoelasticity theory of mixture of two elastic solids, *Journal of Thermal Stresses* **19**(7): 633-648.

[4] Ciarletta M., Scalia A., Svanadze M., 2007, Fundamental solution in the theory of micropolar thermoelasticity for materials with voids, *Journal of Thermal Stresses* **30**(3): 213-229.

[5] Svanadze M., 2005, Fundamental solution in the theory of consolidation with double porosity, *Journal of the Mechanical Behavior of Materials* **16**(1-2): 123-130.

[6] Svanadze M., 2004, Fundamental solutions of the equations of the theory of thermoelasticity with microtemperatures, *Journal of Thermal Stresses* **27**(2): 151-170.

[7] Scarpetta E., Svanadze M., Zampoli V., 2014, Fundamental solutions in the theory of thermoelasticity for solids with double porosity, *Journal of Thermal Stresses* **37**(6): 727-74814.

[8] Svanadze M., 2016, Fundamental solutions in the theory of elasticity for triple porosity materials, *Meccanica* **51**: 1825-1837.

[9] Svanadze M., 2018, Fundamental solutions in the linear theory of thermoelasticity for solids with triple porosity, *Mathematics and Mechanics of Solids* **24**(4): 919-938.

[10] Sharma S., Sharma K., Rani Bhargava R., 2013, Wave motion and representation of fundamental solution in electro-microstretch viscoelastic solids, *Materials Physics and Mechanics* **17**: 93-110.

[11] Sharma S., Sharma K., Rani Bhargava R., 2014, Plane waves and fundamental solution in an electro-microstretch elastic solids, *Afrika Matematika* **25**(2): 983-997.

[12] Kumar R., Sharma K. D., Garg S. K., 2015, Fundamental solution in micropolar viscothermoelastic solids with void, *International Journal of Applied Mechanics and Engineering* **20**(1): 109-125.

[13] Kumar R., Vohra R., Gorla M.G., 2016, Some considerations of fundamental solution in micropolar thermoelastic materials with double porosity, *Archives of Mechanics* **68**(4): 263-284.

[14] Kumar R., Devi S., Sharma V., 2015, Plane wave and fundamental solution in a modified couple stress generalized thermoelastic with mass diffusion, *Materials Physics and Mechanics* **24**: 72-85.

[15] Kumar R., Kansal T., 2011, Fundamental solution in the theory of thermo microstretch elastic diffusive solids, *International Scholarly Research Network ISRN Applied Mathematics* **2011**: 764632.

[16] Kumar R., Kansal T., 2012, Fundamental solution in the theory of micropolar thermoelastic diffusion with voids, *Computational and Applied Mathematics* **31**(1): 169-189.

[17] Kumar R., Kaur M., 2016, Plane waves and fundamental solutions in heat conducting micropolar fluid, *Journal of Fluids* **2016**: 1453613.

[18] Xu F., Lu T., 2011, *Introduction to Skin Biothermomechanics and Thermal Pain*, Berlin (Heidelberg),Springer.

[19] Shen W.S., Zhang J., 2005, Modeling and numerical simulation of bioheat transfer and biomechanics in soft tissue, *Mathematical and Computer Modelling* **41**: 1251-1265.

[20] Shen W.S., Zhang J., Yang F.Q., 2005, Skin thermal injury prediction with strain energy, *International Journal of Nonlinear Sciences and Numerical Simulation* **6**: 317-328.

[21] Li X., Zhong Y., Jazar R., Subic A., 2014, Thermal-mechanical deformation modelling of soft tissues for thermal ablation, *Bio-Medical Materials and Engineering* **24**: 2299-2310.

[22] Li X., Zhong Y., Subic A., Jazar R., Smith J., Gu C., 2016, Prediction of tissue thermal damage, *Technology and Health Care* **2**: 5625-5629.

[23] Xu F., Seffen K., Lu T., 2008, Non-Fourier analysis of skin biothermomechanics, *International Journal of Heat and Mass Transfer* **51**: 2237-2259.

[24] Li X., Zhong Y., Smith J., Gu C., 2017, Non-Fourier based thermal-mechanical tissue damage prediction for thermal ablation, *Bioengineered* **8**(1): 71-77.

[25] Pennes H.H., 1948, Analysis of tissue and arterial blood temperatures in the resting human forearm, *Journal of Applied Physiology* **1**: 93-122.

[26] Cattaneo C., 1958, A form of heat conduction equation which eliminates the paradox of instantaneous propagation, *Journal of Applied Mathematics* **247**: 431-433.

[27] Vernotte P., 1958, Les paradoxes de la theorie continue de l'equation de la chaleur, *Journal of Applied Mathematics* **246**: 3154-3155.

[28] Tzou D.Y., 1995, A unified field approach for heat conduction from macro-to-microscales, *ASME Journal of Heat Transfer* 117: 8-16.

[29] Shrama M.D., 2008, Wave propagation in thermoelastic saturated porous medium, *Journal of Earth System Science* **117**(6): 951-958.

[30] Kupradze V.D., Gegelia T.G., Basheleishvili M.O., Buruchuladze T.V., 1979, *Three Dimensional Problem of Mathematical Theory of Elasticity and Thermo-Elasticity*, North-Holland Publishing, Company Amsterdam, New York, Oxford.

[31] Panji M., Kamalian M., Asgari Marnani J., Jafari M. K., 2013, Transient analysis of wave propagation problems by half-plane BEM, *Geophysical Journal International* **194**: 1849-1865.

[32] Panji M., Kamalian M., Asgari Marnani J., Jafari M. K., 2014, Analysing seismic convex topographies by a half-plane time-domain BEM, *Geophysical Journal International* **197**: 591-607.

[33] Panji M., Ansari B., 2017, Transient SH-wave scattering by the lined tunnels embedded in an elastic half-plane, *Engineering Analysis with Boundary Elements* **84**: 220-230.

[34] Achenbach J.D., 1973, *Wave Propagation in Elastic Solids*, North-Holland Publishing, Amsterdam.

[35] Sharma K., Marin M., 2013, Effect of distinct conductive and thermodynaic temperatures on the reflection of plane waves in micropolar elastic half-space, *UPB Scientific Bulletin, Series A: Applied Mathematics and Physics* **75**(2): 121-132.

[36] Shrama K., 2012, Reflection of plane waves in thermodiffusive elastic half-space with voids, *Multidiscipline Modeling in Materials and Structures* **8**(3): 269-296.

[37] Kumar R., Gupta V., 2013, Reflection and transmission of plane waves at the interface of an elastic half-space and a fractional order thermoelastic half-space, *Archive of Applied Mechanics* **83**: 1109-1128.

[38] Saini R., 2015, Reflection/refraction at the interface of an elastic solid and a partially saturated porous solid containing liquid filled bound pores and a connected pore space saturated by two-phase fluid, *Latin American Journal of Solids and Structures* **12**(10): 1870-1900.
[39] Kumar R., Vohra R., Gorla M.G., 2016, Reflection of plane waves in thermoelastic medium with double porosity, *Multidiscipline Modeling in Materials and Structures* **12**(4): 748-778.